

A model of size-dependent photoluminescence in amorphous silicon nanostructures: Comparison with observations of porous silicon

M. J. Estes and G. Model^{a)}

Department of Electrical and Computer Engineering and the Optoelectronic Computing Systems Center,
University of Colorado, Boulder, Colorado 80309-0425

(Received 12 June 1995; accepted for publication 29 January 1996)

We present calculations using a simple model of radiative recombination in 2D slabs, 1D wires, and 0D spheres of hydrogenated amorphous silicon (*a*-Si:H) showing a significant size dependence of the photoluminescence. Room-temperature peak emission energies >1.8 eV and efficiencies near unity are possible in *a*-Si:H spheres with diameters <20 Å. Broad homogeneous linewidths >0.25 eV are also predicted for these highly confined structures. While the effects are similar to those predicted from quantum confinement, these results are caused by the statistics of spatial confinement. We suggest that these results provide insights into nanostructured *a*-Si:H structures and porous silicon. © 1996 American Institute of Physics. [S0003-6951(96)02213-0]

Efforts to understand the mechanism of visible light emission from porous and nanoscale silicon in terms of a pure quantum confinement model have been complicated by reports of similar luminescence from nanostructured amorphous silicon (*a*-Si). In particular, Bustarret *et al.* reported red-orange light emission from anodically etched and oxidized *a*-Si:B:H films very similar to that observed in identically anodized porous silicon wafers.^{1,2} Lazarouk *et al.* found similar results in anodically oxidized *a*-Si:B:H pillars plasma deposited into porous alumina substrates.³ Because of the localized nature of states in these amorphous structures, quantum confinement effects would be negligible. Thus, another mechanism must be at work in this material.

Even in porous crystalline silicon, there are strong indications for the localized origin of the red-orange luminescence band, including the stretched exponential time decay,^{2,4} the exponential temperature dependence,⁵ the red shift with thermal annealing,⁶ and the correlation of strong luminescence from predominantly amorphous surface layers.^{6,7} Disorder-induced localized states in porous silicon may arise from disordered nanocrystal surfaces⁸ or as amorphous silicon compounds deposited during etching or formed during oxidation.⁹

A number of aspects of porous silicon photoluminescence (PL), though, differ from that in *a*-Si:H. Specifically, the room-temperature peak luminescence energy of *a*-Si:H is less than 1.1 eV (Ref. 10) and is extremely inefficient. Porous silicon, on the other hand, exhibits nominally 1.6–2.0 eV peak energies in the red-orange luminescence band, which is upwards of 10% efficient and relatively independent of temperature. The higher emission energy in porous silicon could be due to alloying with oxygen, nitrogen, or hydrogen,¹¹ but several reports correlate porous silicon luminescence energy with structure size.^{12,13}

In this letter, we apply a simple PL model developed for “bulk” *a*-Si:H and show that by confining amorphous silicon spatially, the luminescence properties change dramatically and become more like those of porous silicon. Although the exact radiative recombination processes involved

in *a*-Si:H are still a matter of debate,¹⁴ existing models of radiative recombination describe reasonably well the luminescence efficiency¹⁰ and the spectral characteristics¹⁵ of the 1.4 eV luminescence band. Our approach is similar to that of Tiedje *et al.*, who fit the observed layer thickness dependence of low-temperature PL due to confinement in one dimension in *a*-Ge:H/*a*-Si:H multilayer films¹⁶ and *a*-Si:H/*a*-Si:N:H multilayers.¹⁷ Here, we consider two-dimensional (2D) slabs, one-dimensional (1D) round wires, and zero-dimensional (0D) spheres of *a*-Si:H, and, using this model, calculate radiative efficiency and luminescence spectra as a function of size.

As illustrated in Fig. 1, photogenerated carriers quickly thermalize to the lowest energy states within some capture radius R_c , before recombining. In this model, radiative recombination takes place via tunneling between deepest accessible energy conduction and valence states without a Stokes shift. In contrast to Dunstan and Boulitrop,¹⁵ we consider the entire *a*-Si:H density of states including both exponential band tail and quadratic band states as potential luminescing sites. Even though the density of states of *a*-Si:H may be size dependent, in this simple model we assume that

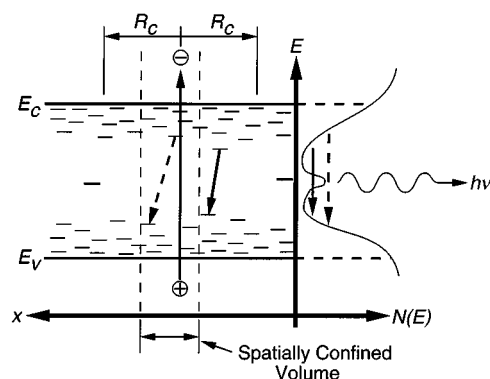


FIG. 1. Diagram showing confined amorphous silicon model. In bulk material, photogenerated carriers thermalize to the lowest energy states, shown as dashes, within the capture radius R_c . Spatially confining carriers to even smaller volumes have the effect of increasing the average energy of the lowest energy state as well as reducing the probability of encountering non-radiative recombination centers, shown as thick dashes.

^{a)}Electronic mail: model@boulder.colorado.edu

it is size independent. We do not consider radiative transitions to or from defect levels near midgap such as the 0.9 eV luminescence band in *a*-Si:H. Non-radiative recombination occurs via tunneling to a nonradiative defect center when such a center is within the capture volume V_c , defined by R_c , or on the surface area A_c , truncating the capture sphere. Finally, we assume that the surfaces do not add additional radiative recombination paths.

We model the strong temperature dependence of the *a*-Si:H PL using an expression for the effective capture radius derived as follows. By equating an expression for the modeled volume radiative efficiency in bulk *a*-Si:H,¹⁰ $\eta = \exp(-V_c N_{nr})$, with the experimentally observed intensity temperature dependence,¹⁸ $\eta = 1/[(1/\eta_0 - 1)\exp(T/T_0) + 1]$, we obtain an expression for $R_c(T)$, which describes the thermal diffusion and tunneling distances. Here, N_{nr} is the volume nonradiative recombination center density, η_0 is the low-temperature maximum quantum efficiency limit, T_0 is an experimentally determined constant, and $V_c = \frac{4}{3}\pi R_c^3$. Using nominal values from Collins *et al.*¹⁸ of $\eta_0 \sim 0.998$ and $T_0 \sim 23$ K along with $N_{nr} \sim 1 \times 10^{16} \text{ cm}^{-3}$ gives a capture radius of ~ 550 Å at room temperature and ~ 70 Å at 40 K.

For a given initial position of the photogenerated electron-hole pair, $R_c(T)$ coupled with the system geometry yields the effective capture volume and surface capture area. We then use the expression given by Tiedje *et al.*¹⁶ for the spatially averaged internal radiative quantum efficiency in a 2D structure, extending it also to the 1D and 0D geometries. The normalized luminescence photon flux spectrum, $P(E)$, is the convolution of the probability density functions of deepest energy conduction and valence band states within the capture volume.¹⁵ Spatially averaging $P(E)$ over the 2D, 1D, and 0D *a*-Si:H structures, taking into account the variation of emission efficiency with position, and multiplying by the photon energy gives the average luminescence intensity spectra $I(E)$, which we compute numerically.

We note that this model oversimplifies the recombination process in *a*-Si:H, particularly at high temperatures. We have assumed that photoexcited electrons and holes diffuse independently. Thus, at high temperatures the pair may be separated well-beyond practical tunneling distances for recombination. In reality, electrons and holes probably do not diffuse independently, and there is probably some correlation between deep states in the conduction and valence band tails. The model does account for the experimentally observed decrease in luminescence energy with increasing temperature.¹⁰ For small capture volumes at low temperatures or in highly confined structures, we expect this model to be reasonably accurate.

In Fig. 2, we show the effect of structure size on room-temperature quantum efficiency for 2D slabs, 1D wires, and 0D spheres of *a*-Si:H with nominal values of the volume and surface nonradiative recombination center densities of $1 \times 10^{16} \text{ cm}^{-3}$ and $1 \times 10^{11} \text{ cm}^{-2}$, respectively. The dip in efficiency between ~ 400 and 1000 Å diam is due to the combination of relatively large surface area *and* relatively large volume of these structures so that carriers are exposed to a maximal number of nonradiative sites. The near-unity quantum efficiency of the small 1D and 0D structures results simply from there being very few states, and therefore, a

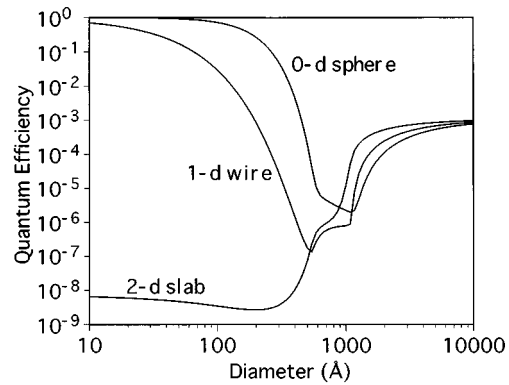


FIG. 2. Predicted internal radiative quantum efficiency vs structure diameter for 2D slabs, 1D wires, and 0D spheres of *a*-Si:H having volume and surface nonradiative recombination center densities of $1 \times 10^{16} \text{ cm}^{-3}$ and $1 \times 10^{11} \text{ cm}^{-2}$, respectively. Efficiencies are calculated based on room-temperature capture radius of 550 Å.

small probability of a nonradiative recombination center, within these volumes.

We show the size dependence of the room-temperature luminescence peak energy for the three geometries in Fig. 3. These data were calculated using a mobility gap of $E_g = 1.7$ eV, conduction and valence band-tail slope energies of 0.026 and 0.043 eV, respectively, and conduction and valence band effective densities of states of $1 \times 10^{21} \text{ cm}^{-3}$. Volume and surface nonradiative recombination center densities are $1 \times 10^{16} \text{ cm}^{-3}$ and $3 \times 10^{10} \text{ cm}^{-2}$, respectively. For comparison, the predicted band gaps in quantum confined silicon crystallites and wires¹⁹ are shown in the inset of Fig. 3. One might imagine a block of *a*-Si:H, having bulk absorption and emission properties, that is sliced into many isolated, smaller pieces. The absorption of the entire set of pieces would be essentially the same as that of the single large block. Because carrier motion would be limited to the volume within each piece, however, the luminescence would blue shift because most carriers would not have access to deeper, and usually distant, gap states. Thus, alloying with hydrogen, oxygen, and/or nitrogen is not required for the higher energy emission. Referring to Fig. 3, we note that

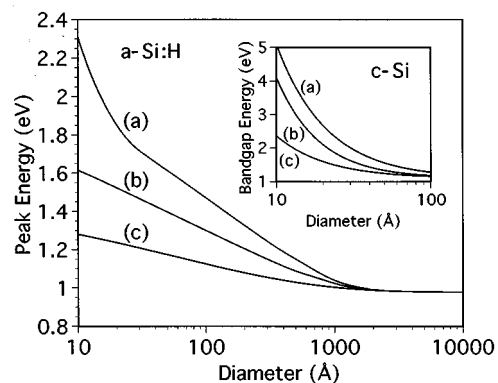


FIG. 3. Predicted room temperature luminescence peak energy vs structure diameter for: (a) 0D spheres, (b) 1D wires, and (c) 2D slabs of *a*-Si:H. Simulation parameters are given in the text. For comparison, inset shows d^{-n} fits to calculated quantum confined silicon band gaps for: (a) crystallites, (b) (100) wires, and (c) (111) wires (see Ref. 19).

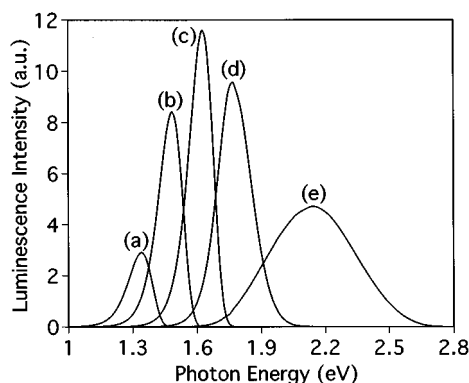


FIG. 4. Simulated room-temperature luminescence intensity spectra for a -Si:H spheres with diameters: (a) 200 Å, (b) 100 Å, (c) 50 Å, (d) 25 Å, and (e) 12.5 Å. Calculation made using same parameters as for Fig. 3.

10–50 Å diam a -Si:H spheres are required to produce the nominally 1.6–2.0 eV porous silicon luminescence. Considering the observed structure sizes in luminescent porous silicon, this size scale is reasonable.

Predicted luminescence intensity spectra for several 12.5–200 Å diam a -Si:H spheres are illustrated in Fig. 4. Larger sized spheres exhibit the asymmetric luminescence peak of bulk a -Si:H while the smaller diameter spheres show a more symmetric peak. The increased width and symmetry of the spectra for these small structures indicates that the lowest energy levels for some structures may be parabolic band states. The spectra exhibit a linewidth of ~ 0.13 – 0.14 eV, which increases to more than 0.25 eV in spheres smaller than 20 Å diam. By comparison, porous silicon linewidths are typically 0.3–0.4 eV. The broad, homogeneous linewidth predicted by our model results from the statistical distribution of states in a -Si:H, not from a distribution of structure sizes, which would further broaden the peak.

We have shown the effects of structure size and shape on the PL properties of a -Si:H nanostructures. By applying a simple model of PL to confined a -Si:H nanostructures, we predict a significant increase in both luminescence intensity and peak energy with confinement, even under our assumptions of size-independent density of states. This effect is due to the statistics of spatial, not quantum, confinement in an

amorphous semiconductor. The simulated luminescence spectra show a broad homogeneous linewidth. Although the origins and morphology of amorphous-like states in porous silicon are still unclear, the red-orange luminescence predicted by this model for highly confined 1D and 0D structures is similar to that of nanostructured amorphous silicon and of porous silicon. Alloying the amorphous silicon with oxygen and/or nitrogen is not required for high energy emission.

We appreciate the financial support of the Materials Research Group and the Colorado Advanced Technology Institute. M. Estes gratefully acknowledges the support of the Air Force Institute of Technology through the Civilian Institute Fellowship Program. We thank J. Pankove, P. Saeta, and R. T. Collins for useful discussions.

- ¹E. Bustarret, M. Ligeon, and L. Ortéga, *Solid State Commun.* **83**, 461 (1992).
- ²E. Bustarret, I. Mihalcescu, M. Ligeon, R. Romestain, J. C. Vial, and F. Madéore, *J. Lumin.* **57**, 105 (1993).
- ³S. Lazarouk, S. Katsuba, N. Kazuchits, G. D. Cesare, S. L. Monica, G. Maiello, E. Proverbio, and A. Ferrari, *Mater. Res. Soc. Symp. Proc.* **358**, 93 (1994).
- ⁴N. Ookubo, *J. Appl. Phys.* **74**, 6375 (1993).
- ⁵R. E. Hollingsworth, C. DeHart, P. K. Bhat, and M. J. Estes (unpublished).
- ⁶S. M. Prokes, J. J. A. Freitas, and P. C. Searson, *Appl. Phys. Lett.* **60**, 3295 (1992).
- ⁷N. Noguchi, K. Suemune, M. Yamanishi, G. C. Jua, and N. Otsuka, *Jpn. J. Appl. Phys.* **31**, L490 (1992).
- ⁸F. Koch, V. Petrova-Koch, and T. Muschik, *J. Lumin.* **57**, 271 (1993).
- ⁹J. C. Tsang, M. A. Tischler, and R. T. Collins, *Appl. Phys. Lett.* **60**, 2279 (1992).
- ¹⁰R. A. Street, in *Semiconductors and Semimetals*, edited by J. Pankove (Academic, New York, 1984), Vol. 21B, p. 197.
- ¹¹B. H. Augustine, E. A. Irene, Y. J. He, K. J. Price, L. E. McNeil, K. N. Christensen, and D. M. Maher (unpublished).
- ¹²L. T. Canham, *Appl. Phys. Lett.* **57**, 1046 (1990).
- ¹³Y. H. Seo, K. S. Nahm, M. H. An, E.-K. Suh, Y. H. Lee, K. B. Lee, and H. J. Lee, *Jpn. J. Appl. Phys.* **33**, 6425 (1994).
- ¹⁴M. Kemp, *1995 Materials Research Society Spring Meeting* (Materials Research Society, Pittsburgh, 1995), paper A3.1.
- ¹⁵D. J. Dunstan and F. Boulitrop, *Phys. Rev. B* **30**, 5945 (1984).
- ¹⁶T. Tiedje, B. Abeles, and B. G. Brooks, *Phys. Rev. Lett.* **54**, 2545 (1985).
- ¹⁷T. Tiedje, *Mater. Res. Soc. Symp. Proc.* **49**, 121 (1985).
- ¹⁸R. W. Collins, M. A. Paesler, and W. Paul, *Solid State Commun.* **34**, 833 (1980).
- ¹⁹C. Delerue, M. Lannoo, and G. Allan, *J. Lumin.* **57**, 249 (1993).